International Journal of Ocean System Engineering 3(2) (2013) 102-110
http://dx.doi.org/10.5574/IJOSE.2013.3.2.102

Study on Mechanical and Thermal Properties of Tio_2/Epoxy Resin Nanocomposites

Bu-Ahn Kim and Chang-Kwon Moon

Department of Materials Science and Engineering, Pukyong National University, Yong dang-dong, Nam-gu, Busan, 608-737, South Korea

(Manuscript Received March 11 2013; Revised April 8, 2013; Accepted M ay 5, 2013)

Abstract

The purpose of this study was to improve the properties of epoxy resin using titanium oxide nanoparticles. The effects of particle weight fraction, dispersion agent, and curing agents with different molecular weights on the thermal and mechanical properties of titanium-oxide-reinforced epoxy resin were investigated. In addition, the effect of the particle dispersion condition on the mechanical properties of nanocomposites was studied.

As a result, it was found that the glass transition temperature of film-shaped nanocomposites decreased with an increase in the nanoparticle content. Because nanoparticles interrupted the cross linkage between the epoxy resin and the amine curing agent, the cross-link density of the epoxy became lower and led to a decrease in T_g in the nanocomposites. The tensile strength and modulus in film-shaped nanocomposites also increased with the particles content. But in the case of dog-bone-shaped nanocomposites, the values were not similar to the trend for the film-shaped nanocomposites. This was probably a result of the different nanoparticles dispersions in the epoxy resins resulting from the respective-thicknesses of the film and dog-bone-shaped samples.

Keywords: Nanocomposites, Cluster, Dispersion agent, Tensile strength, Nanoindentation test, Particle weight fraction, Curing agent, Glass transition temperature (T_g)

1. Introduction

Polymer/inorganic composites have been widely studied as an important source of advanced materials. Polymeric materials are often reinforced by stiff fillers to improve their mechanical properties. The efficiency of the reinforcement depends on the aspect ratio and mechanical properties of the filler, as well as the adhesion between the matrix and the filler.

Over the past several decades, many researchers have focused on polymer nanocomposites because of the potential applicability of the unique properties of these materials in nanosized systems [1-6].

Nanocomposites show much better mechanical properties than similar microsized systems. Because of their very small size, nanoparticles have a high surface-to-volume ratio and provide high-energy surfaces. A desirable result of embedding nanoparticles into a polymer matrix is the enhanced bonding between the polymer matrix and the nanoparticles, resulting from the nanoparticles' high interfacial energy. Classical composite theory predicts that good bonding between the polymer matrix and the

*Corresponding author. Tel.: +82-51-629-6356, Fax.: +82-51-629-6353
E-mail address: moonck@pknu.ac.kr

reinforcing filler leads to improved mechanical properties. For all particle sizes, the composite modulus increases monotonically with the weight fraction of the particles.

However, the strengths of nanocomposites filled with a high weight fraction of particles could be less than the strength of neat resin because of large particle clusters caused by aggregation or agglomeration [7]. One major problem with nanocomposites is the uniform dispersion of nanoparticles in the organic matrix, avoiding macroscopic phase separation. These nanoparticles in the matrix could cause defects and reduce the superior mechanical properties of the nanoparticles in the composites.

The uniform dispersion of nanoparticles in a polymer, with no particle clusters from aggregation and agglomeration, is the most important point in the processing of nanocomposites.

There are various possible methods to prevent aggregation and agglomeration and cause a uniform dispersion. The ordinary ones involve mechanical mixing, ultrasonic vibration, surface treatments, and dispersion agents. If nanoparticles are well dispersed in a polymer, they offer a larger specific surface area compared to the usual fillers, Thus, the potential of these systems is the enhancement of the interfacial interactions between the matrix and the particles, leading to an improvement in the properties of the material [8].

Some authors have reported that a large improvement in the mechanical properties can be achieved at a very low particle content such as 1–5 wt% [9]. In particular, several authors proved that ceramic and silica nanoparticles could be used to effectively reinforce bulk polymers [9, 10].

The enhancement of properties is often seen at particular particle fraction. Many researchers have discovered that the properties decline very sharply as the fraction of particles in a nanocomposite increases above a specific level [11-14]. Therefore, it is necessary to add the particles up to that specific fraction level.

Epoxy resin is a widely used polymer matrix for advanced composites because of its good stiffness, dimensional stability and chemical resistance. Moreover, it is widely used in the industry because of its easy production, light weight, high adhesive property, and so on. The thermal and mechanical properties of epoxy resins are highly dependent on the cross-linked three-dimensional microstructure formed during the curing process.

The purpose of this study was to improve the properties of an epoxy resin using titanium oxide nanoparticles. Therefore, the effects of the particle weight fraction, dispersion agent, and curing agents with different molecular weights on the thermal and mechanical properties of a titanium oxide-reinforced epoxy resin were investigated. In addition, the effect of the particle dispersion condition on the mechanical properties of nanocomposites has been studied.

2. Experimental

2.1 Materials and sample preparation

The following materials were in this study. The titanium dioxide (TiO_2) nanoparticles used were P25 (Evonik Degussa Co.), which had a size of approximately 20 nm according to the manufacturer. There was no surface treatment for the particles. The epoxy resin used was the diglycidyl ether of bisphenol A (DGEBA, Epon 828, Hexion Co.). Three kinds of aliphatic amine curing agents were used to prepare the epoxy matrices: two types of polyoxypropylene diamine (Jeffamine D230, D400) with different molecular weights and polyoxypropylene triamine (Jeffamine T403). The D230 and D400 had average molecular weights of 230 and 400, respectively, and T403 had an average molecular weight of 440. Three kinds of Jeffamine were obtained from Huntsman Corporation, TX, USA, and the dispersion agent was disper180 (Byk Co.).

The film- and dog-bone-shaped samples for the experimental tests of the nanoparticle unfilled and filled composites were prepared using the following procedures. First, two silicone molds with eight dog-bone-shaped cavities and two Teflon plates (100 × 150 × 10 mm) were preheated in an oven at 67^{o}C. The liquid epoxy resin was heated for about 1 h at 67 ^{o}C to lower the viscosity, and then degassed for 30 min in a vacuum oven at 67 ^{o}C. Nanoparticles were measured using a balance (Metter Co., 0.01 mg) and added at 1 wt% and 3 wt%, respectively. They were then mixed for 30 min using a dispermat (Byk-Gardner) at 2000 rpm. After this, the mixture was degassed for 1.5 h in a vacuum oven at 67 ^{o}C, and the curing agent was

added and mixed by hand for 3.0 min using a wooden stick.

The mixture was separated into two 100-cc plastics beakers. One beaker was used for the dog-bone- shaped mold and the other one was used for film forming. The liquid mixture in the beakers was again degassed for 20 min in a vacuum oven at 67 ^{o}C. Afterward, the liquid mixture in one beaker was poured into the preheated dog-bone-shaped silicone mold on the preheated Teflon plate. The other mixture was held in the oven at 67 ^{o}C until it reached the appropriate viscosity to form a film. This waiting time varied with the curing agent, e.g., in the case of the unfilled ones, for D230, D400, and T403, the samples were held in oven at 67 ^{o}C for 30, 70, 35 min after being mixing with the curing agent. In the case of the filled particles, slightly longer times were required compared to the unfilled samples.

The waiting times differed slightly with the weight fraction of the filled nanoparticles and the amount of the mixture. Finally, films were formed on the release paper on the vacuum plate using the draw-down technique. The formed films were cured at room temperature overnight, and then post-cured at 80 ^{o}C for 2 h and 125 ^{o}C for 3 h for a full cure in a forced air circulating oven (Blue M, General Signal Co.). The samples were allowed to cool to room temperature in the oven before removal. The thicknesses of the formed films and dog-bone samples were approximately 90 μm and 2.0 mm, respectively.

2.2 Dynamic mechanical thermal analysis (DMTA)

The storage modulus (E'), loss modulus (E''), and glass transition temperature (T_g) of the films were measured using a dynamic mechanical analyzer (TA Instrument, RSA III). Rectangular samples (30 mm × 4 mm) were cut from the films using a clean razor blade. The gauge length of a sample was 15 mm. The samples were tested from -130 ^{o}C to 130 ^{o}C using a strain of 0.01, frequency of 1 Hz, and temperature ramp of 3 ^{o}C min^{-1}. The T_g was determined from the peak position in tan δ (defined as E''/ E'). The storage modulus at -50 ^{o}C is reported. The reported values for T_g and E' were the averages from the four samples.

2.3 Tensile Tests

Table 1. T_g of nanocomposites cured using D230

Materials	T_g (℃)
D230	90.5
D230 - 1wt% TiO_2	88.6
D230 – 1wt% TiO_2 BYK 180	86.5
D230 – 3wt% TiO_2 BYK 180	84.5

Tensile tests of the films were performed using a dynamic mechanical analyzer in tensile test mode (TA Instrument, RSA III) in accordance with the ASTM D638-08 test standard. The samples were 63.5 mm long, 9.53 mm wide all over, and 3.18 mm wide in the narrow section. The strain was measured using grip separation. The apparent Young's modulus was determined from the slope of the linear portion of the engineering stress vs. engineering strain curve. All of the tensile test specimens were conducted at a constant cross head speed of 1.0 mm/min and a gauge length of 15 mm. The modulus and tensile strength were averaged from 7 samples.

Before the testing, the upper side of a dog-bone-shaped sample was polished to make a flat surface, and the edges of the sample were polished using sand paper with a mesh of #1200. The tensile tests of the dog-bone-shaped samples were carried out using a tensile tester (Instron Co.) with a 1-KN load cell. The cross-head speed was 1.0 mm/min, with a gauge length of about 15 mm. The strain was measured using a video strain measurement meter. The samples were 60.92 mm long, 10.65 mm wide all over, and 4.0 mm wide in the narrow section. The reported modulus and tensile strength were averaged from 10 samples.

2.4 Microscope observation

An optical microscope was used to observe the nanoparticle dispersions in the films. A cover glass and oil with a refraction index of approximately 1.50 were used to improve the image clarity. The refraction index of the oil was almost the same as that of the matrix resin used in this study. The oil flowed to fill the entire contact area between the film and the cover glass.

A laser scanning confocal microscope (LSCM, Zeiss model LSM510) was also used to observe the nanoparticle dispersions on the surfaces and subsurfaces of the films and dog-bone-shaped samples.

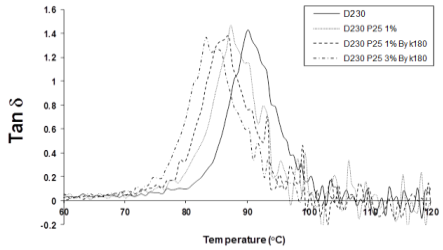

Fig. 1 Tan δ and Temperature of film-shaped samples

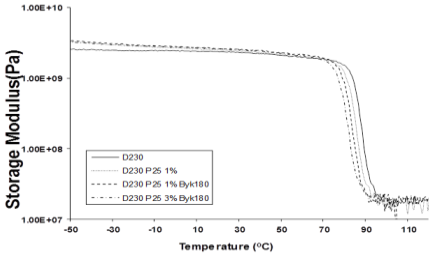

Fig. 2 Storage modulus vs. temperature of film-shaped samples

The laser wavelength used in this study was 543 nm. The LSCM images presented in this paper are two-dimensional (2D) intensity projections and a single depth-profile image at a particular z-depth (depth-profile image). The 2D LSCM image is formed by summing stacks of images in the *z* direction; (512 pixel x 512 pixel) of the film-shaped and dog-bone-shaped samples. The pixel intensity level represents the total amount of back-scattered light. Darker areas represent regions that scattered less light than lighter the colored areas.

3. Results and discussion

3.1 Dynamic mechanical thermal analysis (DMTA)

The results of DMTA tests of the pure epoxy and TiO_2/epoxy nanocomposites are shown in Figs. 1−4.

Figs. 1 shows the relationships between tan δ and the temperature of the film-shaped pure epoxy and the nanocomposites. These were cured by Jeffamine D230, and nanoparticles were added at 1 wt% (with or without dispersant Byk180), and 3 wt%. In this study, the peak temperature of the tan δ is applied to define the glass transition temperature (T_g) and the values are given in Table 1.

As shown in Table 1, T_g decreased with an increase in the nanoparticle weight fraction. It can be explained that the nanoparticles prevented the cross linkage between the epoxy resin and the amine curing agent, which induced a lower epoxy cross-link density in the nanocomposites compared to the pure epoxy. It was reported that nanoparticles can significantly alter the thermal and mechanical properties of a polymer close to the particle surface because of changes in the polymer chain mobility [7, 15-16]. When 1 wt% nanoparticles were added, the T_g of the sample with dispersant Byk180 was lower than the one with no dispersant. This very clearly showed the dispersant effect. That is, the dispersion status of the sample with dispersant was better than the one with no dispersant, as can be seen in Fig. 18.

Fig. 2 presents the storage modulus versus temperature of the film-shaped pure epoxy and nanocomposites. These were cured using Jeffamine D230, and nanoparticles were added at 1 wt% (with or without dispersant Byk180) and 3 wt%. In this figure, the storage modulus in the glassy region was slightly higher than that of the pure epoxy. However, around T_g, the values were the opposite.

Fig. 3 reveals the relationships between tan δ and the temperature of the film-shaped pure epoxy and nanocomposites, which were cured using Jeffamine D400. In this figure, the T_g of the nanocomposites is lower than that of pure epoxy.

Fig. 4 shows the tan δ according to the temperature of the film-shaped pure epoxy and nanocomposites, which were cured using Jeffamine T403. In this figure, the T_g of the nanocomposites is lower than that of the pure epoxy.

In Figs. 3, and 4, although curing agents with high molecular weights were used, the T_g values of the nanocomposites are lower than that of the pure epoxy, as shown in Fig. 1. Therefore, it is considered that the nanoparticles added to the epoxy resin obstructed the cross-linkage between the epoxy resin and the amine curing agent, which could eventually affect the T_g of the nanocomposites, regardless of the molecular weight of the curing agent.

3.2 Tensile tests

Film-shaped and dog-bone-shaped samples were used in the tensile tests, and the results for the film-shaped samples are shown in Figs. 5−8.

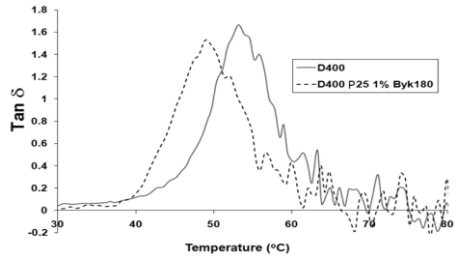

Fig. 3 Tan δ and temperature of film-shaped samples

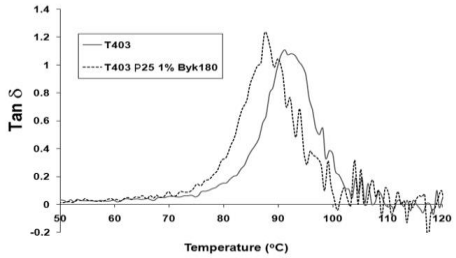

Fig. 4 Tan δ and temperature of film-shaped samples

Fig. 5 presents the tensile strengths of the film-shaped pure epoxy and nanocomposites. Both were cured by Jeffamine D230, and the nanoparticles were added at 1 wt% (with or without dispersant Byk180) and 3 wt% with dispersant Byk 180. As seen in this figure, the tensile strengths of the nanocomposites were higher than that of the pure epoxy, and the tensile strength increased with nanoparticle content. The tensile strength of the 1wt% filled nanocomposites with dispersant Byk 180 was higher than the one with no dispersant. It was found that the use of Byk180 as a dispersant was very effective at improving the dispersion of the TiO_2 nanoparticles in the epoxy resin.

Fig. 6 shows the tensile moduli of the film-shaped pure epoxy and nanocomposites, both of which were cured using Jeffamine D230, and nanoparticles were added at 1 wt% (with or without dispersant Byk180) and 3 wt%.

As seen in this figure, the tensile moduli of the nanocomposites were higher than that of the pure epoxy, and the tensile modulus increased with the nanoparticle content. The tensile modulus of the 1 wt% filled nanocomposites with dispersant Byk180 was higher than the one with no dispersant.

This is consistent with the trend for the tensile strength. This probably occurred because the better dispersion of the nanoparticles in the nanocomposites could improve the tensile properties.

Fig. 7 reveals the tensile strengths of the film-shaped pure epoxy and nanocomposites, which were cured using Jeffamine D230, D400, and T403, and all of the nanocomposites were filled with 1 wt% Byk180.

Only the tensile strength of the nanocomposites cured using Jeffamine D230 was higher than that of the pure epoxy, while the others were not. However, in the case of the tensile moduli even with the same sample, the values for the nanocomposites were higher than those of the pure epoxy, as shown in Fig. 8.

The results of the tensile tests in dog-bone-shaped samples are shown in Figs. 9−12.

Fig. 9 shows the tensile strength of the dog-bone-shaped pure epoxy and nanocomposites. These were cured using Jeffamine D230, and the nanocomposites were filled with dispersant Byk180 at 1 wt% and 3 wt%.

As seen in this figure, the tensile strengths of all the nanocomposites were slightly lower than that of the pure epoxy. The tensile strengths of 1 wt% and 3 wt% filled nanocomposites with dispersant Byk180 were slightly higher than that of the 1 wt% nanocomposites with no dispersant.

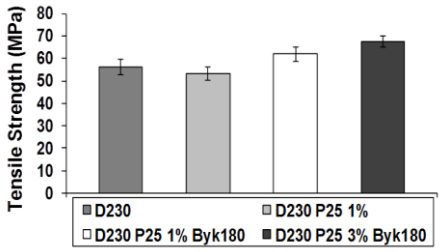

Fig. 5 Tensile strength of film-shaped samples

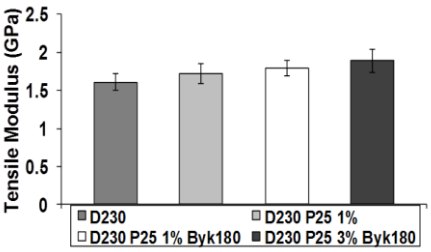

Fig. 6 Tensile modulus of film-shaped samples

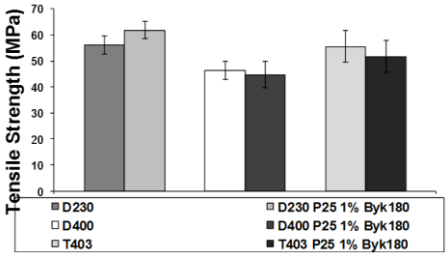

Fig. 7 Tensile strength of film-shaped samples with different curing agents

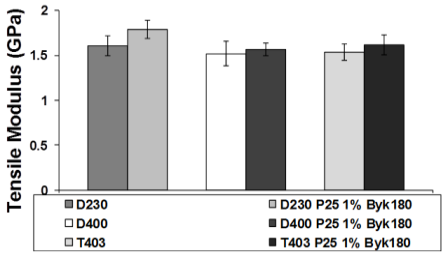

Fig. 8 Tensile modulus of film-shaped samples with different curing agents

Fig. 10 shows the tensile moduli of the dog-bone-shaped pure epoxy and nanocomposites. These were cured using Jeffamine D230, and the nanocomposites were filled with dispersant Byk180 at 1 wt% and 3 wt%.

As shown in this figure, the tensile moduli of all the nanocomposites were higher than that of the pure epoxy, but the tensile modulus did not increase with the nanoparticle content like the film-shaped samples, as can be seen in Fig. 6.

Fig. 11 reveals the tensile strengths of the dog-bone-shaped pure epoxy and nanocomposites, which were cured using Jeffamine D230, D400, and T403, while all the nanocomposites were filled with 1 wt% and Byk180.

The tensile strengths of all the dog-bone-shaped nanocomposites were lower than those of the pure epoxy. However, in the case of the tensile moduli even with the same sample, the values of the nanocomposites were higher than those of the pure epoxy, as shown in Fig. 12. In Figs. 5, 6, 9, and 10, there are significantly different results between the film-shaped and dog-bone-shaped samples. In the film-shaped samples, the tensile strengths of the nanocomposites were higher than that of the pure epoxy, and the tensile strength increased with the nanoparticle content. The tensile moduli of the nanocomposites were higher than that of the pure epoxy and increased with increasing nanoparticle content.

In the dog-bone-shaped samples, the tensile strengths of all the nanocomposites were lower than that of the pure epoxy.

The tensile moduli of the nanocomposites were higher than that of the pure epoxy, but they did not increase with the nanoparticle content like the film-shaped nanocomposites. This was presumably a result of the non-uniform dispersion condition of the nanoparticles in the epoxy resulting from the different dimensions of the film- and dog-bone-shaped samples, as can be seen in Fig. 20. As described in the experimental section, the thicknesses of the film and dog-bone samples were approximately 90 μm and 2.0 mm, respectively.

3.3 Microscope observations

The overall degree of dispersion could be determined using the optical microscope.

Fig. 13 shows optical microscope photos of the upper sides of the film-shaped samples that were cured using Jeffamine D230, and nanocomposites were filled with 1 wt% (a), and 1 wt% and 3 wt% with dispersant Byk180 (b, c). As can be seen in this figure, the macroscopic dispersions of all the samples were almost uniform, but the microscopic dispersions were non-uniform.

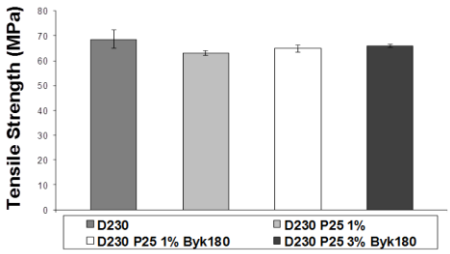

Fig. 9 Tensile strength of dogbone-shaped samples

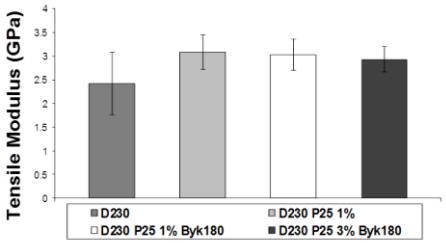

Fig. 10 Tensile modulus of dogbone-shaped samples

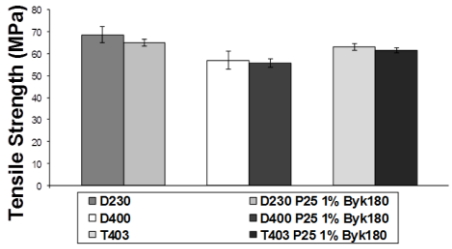

Fig. 11 Tensile strength of dogbone-shaped samples with different curing agents

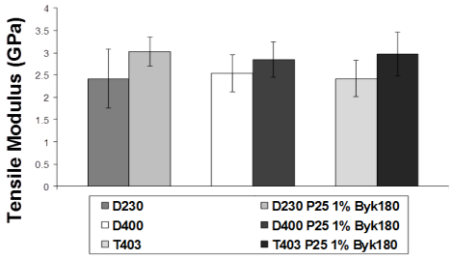

Fig. 12 Tensile moduli of dog-bone-shaped samples with different curing agents

Comparing (a) with (b), in spite of using the same weight fraction of TiO_2, the cluster sizes and numbers are different. The dispersion status of the nanoparticles in the sample with dispersant was better than that of the sample with no dispersant. There were large particle clusters of about 10~20 μm. In the case of (c), there were larger clusters than (b).

Fig. 14 presents optical microscope photos of a film-shaped sample that was cured using Jeffamine D230 and filled with 3 wt% Byk180. Those photos show the dispersion status of the nanoparticles on the upper side and bottom side surface of the film-shaped sample. As can be seen in this figure, large big clusters were formed to a greater degree on the bottom side (b) than the upper side (a) of the film. This shows to difference in the degrees of dispersion between the upper side and bottom side of the film-shaped nanocomposites.

Fig. 15 shows nanoparticle dispersion photos of the 4-μm subsurface obtained using laser scanning confocal microscope. It shows the dispersion status of the upper side and bottom side layer of the dog-bone- shaped sample, which was cured using Jaffamine D230 and filled with 3wt% Byk180. These images show the dispersion of the nanoparticle clusters in the subsurface layers of the nanocomposites. Larger particle clusters were observed on the bottom side of the dog-bone-shaped sample than the upper side of the sample. This was supposed to be the reason for the different values caused by the different dimensions between the film and dog-bone-shaped samples in the tensile tests as shown in Figs. 9−12.

In Figs. 14 and 15, the dispersion situation of the nanoparticles in the film-shaped sample with 3 wt% Byk180 was better than that of the dog-bone-shaped sample, and the dispersion situations of the nanoparticles between the upper and bottom sides of the film-shaped sample were slightly different, while the dispersion situations of the nanoparticles between the upper and bottom sides of the dog-bone-shaped sample were distinctly different. Compared with the upper side of dog-bone-shaped samples, many large clusters were found on the bottom side, like from aggregation or agglomeration.

4. Conclusion

The purpose of this study was to improve the properties of epoxy resin using titanium oxide nanoparticles. Therefore, the effects of the particle weight fraction, dispersion agent, curing agents with different molecular weights and specimen shape on the thermal and mechanical properties of a titanium oxide nanoparticle-reinforced epoxy resin were investigated. In addition, the effect of the particle dispersion situation on the mechanical properties of nanocomposites has been studied. The results were as follows.

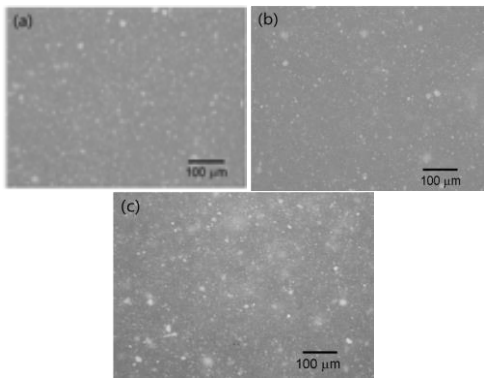

Fig. 13 Optical microscope photos of upper side of film-shaped samples: (a) 1 wt% (b) 1 wt% Byk180 (c) 3 wt% Byk180

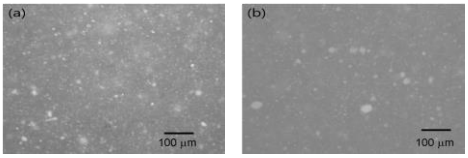

Fig. 14 Optical microscope photos of film-shaped samples with 3 wt% Byk 180: (a) upper side and (b) bottom side

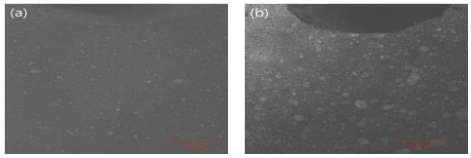

Fig. 15 Particle dispersion photos of 4 μm subsurface obtained using laser scanning confocal microscope on dog-bone-shaped sample with 3 wt% Byk 180: (a) upper side layer and (b) bottom side layer

1. The T_g of nanocomposites decreased with increasing nanoparticle content. Because the nanoparticles interrupted the cross linkage between the epoxy resin and the amine curing agent, the cross-link density of the epoxy became lower, which led to a decrease in the T_g of the nanocomposites.

2. The tensile strength and modulus of the film-shaped nanocomposites increased with the nanoparticle content. However, in the case of the dog-bone-shaped nanocomposites, the values were not similar to the trend for the film-shaped nanocomposites. This was probably because of the different dispersion status of the nanoparticles in the epoxy resin resulting from the different dimensions between the film and dog-bone-shaped samples.

3. The dispersion status of the nanoparticles in the film-shaped sample with dispersant was better than the one with no dispersant. In addition, the dispersion degrees of the upper and bottom sides of the film-shaped nanocomposites were slightly different. However, the dispersion situations for the upper and bottom sides in dog-bone-shaped nanocomposites were distinctly different. In other words, large clusters were formed in the dog-bone-shaped nanocomposites much more readily on the bottom side than on the upper side. This is supposed to be the reason for the large scattering of the values in the measured mechanical properties.

References

[1] Vollenberg, P. H. T, Heikens, D. Particle size dependence of the Young's modulus of filled polymers: 1. Preliminary experiments, Polymer 30 (1989) 1656-1662.

[2] Chan, C.-M., Wu, J., Li, J.-X., Cheung, Y.-K. Polypropylene/calcium carbonate nanocomposites, Polymer 43 (2002) 2981-2992.

[3] Su, S., Jiang, D. D., Wilkie, C. A. Methacrylate modified clays and their polystyrene and poly(methyl methacrylate) nanocomposites, Polymers for Advanced Technologies 15 (2004) 225-231.

[4] Park, J. H., Jana, S. C. The relationship between nano- and micro-structures and mechanical properties in PMMA–epoxy–nanoclay composites, Polymer 44 (2003) 2091-2100.

[5] Gersappe, D. Phys. ReV. Lett. Molecular Mechanisms of Failure in Polymer Nanocomposites, Phys. Rev. Lett 89 (2002) 8301-8303.

[6] Reynaud, E., Jouen, T., Gauthier, C., Vigier, G., Varlet, J Nanofillers in polymeric matrix: a study on silica reinforced PA6, Polymer 42 (2001) 8759-8768.

[7] Ash, B. J., Richard, W. S., Linda, S. S. Mechanical Behavior of Alumina/Poly(methyl methacrylate) Nanocomposites, Macromolecules 37 (2004) 1358-1369.

[8] Schmidt, D., Shah, D., Giannelis, E. P. New advances in polymer/layered silicate nanocomposites, Current Opinion in Solid State and Materials Science 6 (2002) 205-212.

[9] Wetzel, B., Haupert, F., Zhang, M. Q. Epoxy nanocomposites with high mechanical and tribological performance, Composites Science and Technology 63 (2003) 2055-2067.

[10] Wang H., Bai Y., Liu S., Wu J., Wong C. P. Combined effects of silica filler and its interface in epoxy resin, Acta Materialia 50 (2002) 4369-4377.

[11] Ou, Y., Yang, F., Yu, Z. A new conception on the toughness of nylon 6/silica nanocompo-

site prepared via in situ polymerization, Journal of Polymer Science Part B: Polymer 36 (1998) 789-795.

[12] Becker, C., Krug, J., Schmidt, H. Tailoring of Thermomechanical Properties of Thermoplastic Nanocomposites by Surface Modification of Nanoscale Silica Particles, MRS Proceedings 435 (1996).

[13] Ash, B. J., Stone, J., Rogers, D. F., Schadler, L. S., Siegel, R. W., Benicewicz, B. C., Appl, T. Investigation into the Thermal and Mechanical Behavior of PMMA/Alumina Nanocomposites Materials Research Society Symposium Proceedings 661 (2001)

[14] Ng, C. B., Ash, B. J., Schadler, L. S., Siegel, R. W. A study of the mechanical and permeability properties of nano- and micron-TiO2 filled epoxy composites, Advanced Composites Letters 10 (2001) 101-111.

[15] Lee, J. Y., Su, K. E., Chan, E. P. Impact of Surface-Modified Nanoparticles on Glass Transition Temperature and Elastic Modulus of Polymer Thin Films, Macromolecules 40 (2007) 7755-7757.

[16] Ciparari, D., Jacob, K., Rina, Tannenbaum, R. Characterization of Polymer Nanocomposite Interphase and Its Impact on Mechanical Properties, Macromolecules 39 (2006) 6565-6573.